

# Discharge Coefficients and on-axis Flow Properties in Small Sonic Orifices at Low Reynolds Numbers

G. Koppenwallner\*, T. Lips\*, C. Dankert\*\*

\*HTG, Max Planck Strasse 19, 37191 Katlenburg Lindau, Germany

\*\*DLR, Bunsenstrasse 10, 37073 Göttingen, Germany

**Abstract.** Sonic nozzles serve as important elements for the generation of supersonic free jets. Sonic nozzles are also used for the generation of well defined mass flow rates for gas metering and as mass flow calibration standards. Small nozzles with a well defined inlet contour are difficult to manufacture. We therefore concentrated our study on simple orifice type nozzles, which have only two geometric dimensions namely the diameter  $D$  of the cylindrical cross section  $d$  and the cylindrical length  $L$ . In this study we combine unpublished experimental data of DLR with new mass flow measurements conducted by HTG in order to give a systematic overview of the flow development in short sonic orifices. The experimental study covers a geometric  $L/D$  range of  $0 < L/D < 7$  with Reynolds numbers between  $50 < Re_D < 25000$ .

## INTRODUCTION

Sonic nozzles serve as important elements for the generation of supersonic free jets [1]. Sonic nozzles are also used for the generation of defined mass flow rates and as mass flow calibration standards [2]. Discharge coefficients  $c_D$  for Ideal orifices with  $L/D = 0$  have been extensively investigated for the complete Knudsen number range. The first comprehensive investigation was conducted by Liepmann [3]. The most systematic experimental study was conducted by Naumann, Chun and partially presented at the 9<sup>th</sup> RGD symposium [4]. Unfortunately Chun's excellent experimental data did not find the deserved attention in the scientific community. For contoured small orifices the work of Kuloya [5] and Fenn, Tang [6] deserves attention. Of major importance is the numerical work of Sharipov [7], who studied the flow through orifices with DSMC methods. Sharipov also gives a good review on previous studies, missing however Chun's work. Chun's experimental data show that the discharge coefficient has in the rarefied transition regime a slight maximum at  $Kn = 0.01$ , which is also indicated by Liepmann's results. Sharipov's DSMC results fail however to show this maximum.

The free molecular flow through cylindrical short orifices with  $L/D > 0$  was originally solved by the classical work of Clausing [8] by introduction of transmission probabilities. However it has to be remembered that in contrast to ideal orifice flow, the gas surface interaction can strongly influence transmission probabilities and flow rates. The continuous effort of Sreekanth [9], whose studies cover the experimental and theoretical analysis of rarefied flow through short ducts, deserves attention. In subsonic continuum flow, an older study by Hansen [10] could be found, where the influence of corner radius and  $L/D$  on the contraction were investigated for  $L/D < 1$ . These studies covered Reynolds number of 2500 - 90 000. Due to recent interest in micro thrusters Gimmelshein et al. [11] studied experimentally and numerically the transitional flow in short cylindrical orifices. Their results cover  $L/D$  between 0.015 and 1.5 and the Knudsen number range between  $Kn = 40$  and 0.0034. Unfortunately only mass flow and specific impulse rates are given in their publication, which do not allow an evaluation of exact discharge coefficients. The DSMC analysis of orifice flow by Danilatos [12] also deserves attention. In the present study we approach the subject experimentally from the continuum side.

## THE NOZZLE GEOMETRIES

One sonic nozzle set for mass flow and one nozzle set for on-axis flow property measurement have been used.

### Nozzles for mass flow and discharge coefficient measurements

These nozzles had nominal diameters of  $D = 2$  mm with length between  $L = 0.25$  and 14 mm. The following Table 1 summarizes the data of all nozzles. The table gives the diameters for nozzle entrance and nozzle exit, which were measured with a microscope to an accuracy of  $\pm 0.002$  mm. Nozzle front- and backsides were grounded in order to

ensure a sharp 90° entry corner. Figure 1 shows the details of the 2 mm nozzle. The nozzles could be inserted into a nozzle holder with two KF 16 flanges, which allowed the installation between air supply and the downstream vacuum tank, with a volume of 0.54 m<sup>3</sup> and a two stage vacuum pump having 45 m<sup>3</sup>/h suction capability . This assured for all tests choked flow conditions. A photograph of all nozzles and nozzle holder is shown in Fig.2. The contraction ratio between air supply tube and sonic orifice was  $m = (D^*/D_{\text{supply}})^2 = (2/12)^2 = 0.0278$ . This corresponds to a Mach number of  $Ma = 0.016$  and a pressure ratio of  $p/p_0 = 0.99982$ . Thus the measured pressure in the supply tube can be set equal to the stagnation chamber (source) pressure.

#### Nozzle for on axis flow property measurements

The nozzles for these tests had diameters of  $D = 15$  mm. Table 1 summarizes also the geometric data of these nozzles. Tests were conducted at  $p_0 = 133.3$  mbar and at ambient temperature with  $p_0 \cdot D = 2000$  mbar,mm.

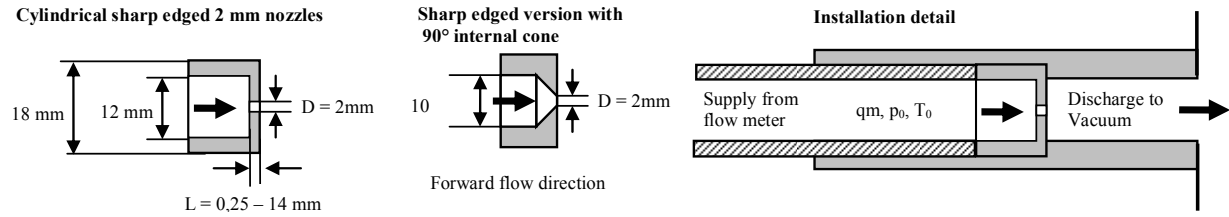


**Fig. 1 Sketch of cylindrical nozzle geometries**

**Table 1 Geometric data of nozzles**

Geometric data of nozzles		$D_{\text{Inlet}}$	$D_{\text{Exit}}$	$L$		
Task / nozzle series	No	mm	mm	mm	L/D	Position
Mass flow 2mm nozzles	1	2.032	2.042	0.240	0.12	front side/back side
	2	1.994	1.987	0.470	0.236	front side/back side
	3	2.011	2.046	1.020	0.50	front side /back side
	4	1.998	2.026	2.015	1.00	front side /back side
	5	2.003	2.013	4.100	2.05	front side /back side
	6	2.046	2.000	8.010	4.00	front side /back side
	7	2.018	2.048	13.800	6.80	front side /back side
Nozzle with $L/D = 0$ conical entrance	8	2.065	2.065	0	0	front side; 90° cone backside; 180° flat
On axis flow static p	1	15.00	15.00	0.15	0.10	front & backside
Pitot $pt_2$	2	15.00	15.00	3.75	0.25	front & backside
15 mm nozzles	3	15.00	15.00	7.50	0.50	front & backside
	4	15.00	15.00	15.00	1.00	front & backside
	5	15.00	15.00	30.0	2.00	front & backside

## THE EXPERIMENTAL SET UP.

### Set up for discharge coefficient measurement

The set up for these experiments is sketched in Fig 2. Air is supplied via 3 Laminar Flow Meters LFM and a throttling valve, which allows the pressure  $p_0$  to be adjusted. Due to the large mass flow range 3 high precision Laminar Flow Meters with accuracy  $\Delta q_v/q_v < 0.1\%$  were used.

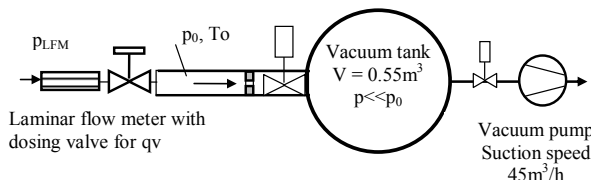


**Fig. 2 Principal set up for discharge coefficient measurement**

The flow meters were operated at a pressures  $p_{\text{LFM}}$  close to atmospheric conditions. Volume flow,  $q_v$ , and mass flow,  $q_m$ , through the orifice were calculated using mass conservation between the flow meter and orifice:  $p_{\text{LFM}} \cdot q_{v,\text{LFM}} = p_0 \cdot q_{v,0}$ . For pressure measurement MKS Baratron's have been used. The calibration constant,  $E_K$ , and accuracy of the flow meters are

given in Table 2. Mass flow measurements were conducted with air at ambient temperature covering a  $p_0 \cdot D$  range of  $3 \text{ mbar} \cdot \text{mm} < p_0 \cdot D < 2000 \text{ mbar} \cdot \text{mm}$ .

**Table 2 Reference laminar flow meters and characteristics**

LFM Flow Meter	$E_k = qv/Dp; (\text{l/min})/\text{mb}$	Accuracy %
Lam AL 50-10	4.8783	0.305%
Lam AL 10-10	1.015	0.28%
Lam 1-10	0.09272	0.146%

### The set up for on-axis flow profiles

The large orifices with  $D = 15 \text{ mm}$  allowed measurements with small diameter probes of the flow properties inside the nozzles. For these tests a cylindrical static probe and a Pitot probe were used. The static probe was a movable cylindrical tube with 2 mm diameter. The tube had one orifice for pressure sensing. The probe was aligned on-axis by two supports. The probe with pressure tap could be moved from the stagnation chamber through the orifice into the exhausting free jet. Fig. 3 shows this set up. The Pitot tube was mounted on the vacuum side on a movable support and allowed measurements from the stagnation chamber through nozzle into the free jet. The experiments were conducted in the DLR Goettingen Vacuum Tunnel [13]. The large suction speed of the vacuum pumps allowed tests on these scaled up- sonic orifices.

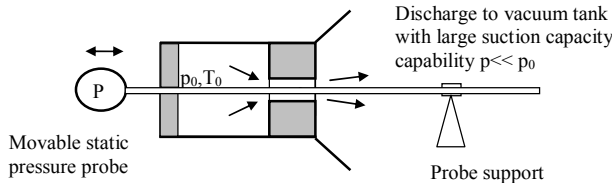


**Fig. 3 Set up for axial flow profile measurement**

## A SHORT REVIEW OF THEORETICAL BACKGROUND

### Ideal orifice flow in the continuum limit

Stream tube gas dynamics gives a simple formula for mass and volume flow through sonic orifices with  $L/D = 0$ .

$$qm = \frac{\pi}{4} D^2 \frac{p_0}{\sqrt{RT_0}} \Gamma(\kappa); \quad qv = \frac{\pi}{4} D^2 \sqrt{RT_0} \Gamma(\kappa) \quad \text{with} \quad \Gamma(\kappa) = \sqrt{\kappa(2/(\kappa+1))^{\frac{\kappa+1}{\kappa-1}}}$$

When approaching the subject from the continuum side the flow rates calculated with these equations are used for normalization of actual flow rates into a discharge coefficient  $C_D$ . The discharge coefficient is defined by:

$$C_D = qv_{\text{actual}} / qv_{\text{idealstreamtube}}$$

It is well known that, due to the sharp entrance, a flow contraction occurs at the continuum limit reducing the geometric throat diameter,  $D$ , to an effective throat diameter,  $D_{\text{eff}}$ . This effect is usually considered by using the discharge coefficient definition.

### Ideal orifice flow in the free molecular limit

The free molecular effuse flow [4] through an orifice with backpressure  $p_b \ll p_0$  is given by:

$$qm_{FM} = \frac{\pi}{4} D^2 \frac{1}{\sqrt{2\pi}} \frac{p_0}{\sqrt{RT_0}}; \quad qv_{FM} = \frac{\pi}{4} D^2 \frac{1}{\sqrt{2\pi}} \sqrt{RT_0}.$$

The discharge coefficient of free molecular orifice flow is therefore given by:

$$c_{D,FM} = \frac{qv_{FM}}{qv_{\text{idealstreamtube}}} = \frac{1}{\sqrt{2\pi}} \frac{1}{\Gamma(\kappa)}.$$

When approaching the subject from the molecular limit, a reduced mass flow rate,  $W = qv/qv_{FM}$  is often defined by use of the free molecular flow rate, e.g. Sharipov [5].

### Cylindrical orifices with finite $L/D$

In the continuum limit no analytic solution is available. In free molecular flow the solution is based on the ideal orifice  $L/D = 0$  with a correction for the transmission probability,  $P(L/D)$ , and can be written in the following way:

$$qv(L/D) = qv(L/D = 0) * P(L/D)$$

where  $qv(L/D=0)$  represents the volume flow entering a control area at the duct inlet and  $P(L/D)$  represents the transmission probability for the entering particle flow. The transmission probability  $P(L/D)$  was originally determined by Clausing [8].

### Reynolds- and Knudsen number definitions

The characteristic Reynolds number  $Re_{D,0}$  for sonic orifice flow is usually defined as:

$$Re_{D,0} = \frac{\rho^* a^* D}{\mu(T_0)} = \frac{D}{\mu(T_0)} \frac{p_0}{\sqrt{RT_0}} \Gamma(\kappa); \text{ With } \rho^*, a^* \text{ density, velocity at sonic throat conditions } a^* = V^*.$$

We base Knudsen number on the Maxwellian mean free path,  $\lambda_0$ , at stagnation chamber conditions and obtain then

$$Kn_0 = \frac{\lambda_0}{D} = \frac{16}{5} \frac{1}{\sqrt{2\pi}} \frac{\mu_0}{\sqrt{RT_0}} \frac{RT_0}{p_0} \frac{1}{D}.$$

We can establish the following relation between  $Kn_0$  and  $Re_{D,0}$

$$Kn_{D,0} = \frac{16}{5} \frac{1}{\sqrt{2\pi}} \frac{\Gamma(\kappa)}{Re_{D,0}}; \quad Kn_{D,0} = 0,8741/Re_{D,0} \text{ for } \kappa = 1.4 \text{ and } G(\kappa) = 0,6847$$

## RESULTS OF DISCHARGE COEFFICIENT MEASUREMENTS

### Selection of reference diameter for discharge coefficient

The discharge coefficient is extremely sensitive to the measured nozzle diameter  $D$ . A 1% error in  $D$  gives a 2 % error in the discharge coefficient. Due to manufacturing inaccuracies we had differences in nozzle diameters between the inlet and exit section of  $\Delta D \leq 0.04$  mm. For each nozzle these diameters were measured in 2 orthogonal directions at the entrance and in 2 orthogonal directions at the exit. With these 4 measurements one can define a mean diameter at the nozzle front side (nominal inlet),  $D_{\text{front side}}$ , a mean diameter at the nozzle back side (nominal exit),  $D_{\text{back side}}$ , or a mean diameter,  $D_{\text{mean}}$ , considering in- and outlet values. To find the physical relevant diameter position we tested the nozzles in forward and backward flow direction and calculated from measured mass flow rates the discharge coefficients in the following three ways: 1. forward flow with  $D_{\text{ref}} = D_{\text{front side}}$ ; 2. backward flow with  $D_{\text{ref}} = D_{\text{back side}}$ ; 3. backward flow with  $D_{\text{ref}} = D_{\text{front side}}$ . For a geometrically perfect nozzle forward and backward results should be identical.

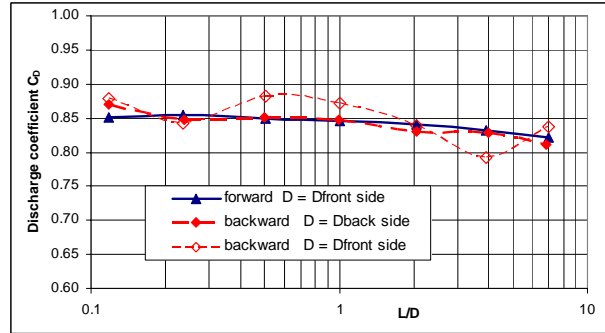


**Fig. 4 Influence of diameter selection on discharge coefficient  $C_D$ ; 2 mm nozzle at  $Re_D = 25000$**

The experimental results in Figure 4 show, that the backward discharge coefficient matches the forward  $C_D$  results in the case where  $D_{\text{backside}}$  is selected as reference. If we base the evaluation of forward, backward measurements on the same mean diameter,  $D$ , we observe a large scatter for cases with small differences between  $D_{\text{front side}}$  and  $D_{\text{back side}}$ .

The results demonstrate that for flow contraction and the resulting  $C_D$  the entrance of the nozzle is relevant. Therefore the diameter of the actual nozzle inlet section served as a reference for all later tests. The experiments show that in the high Reynolds number limit the discharge coefficient of flat-faced orifices has a value of  $C_D = 0.85$ , which is in agreement with other investigations e.g. Sharipov [7]. Surprising is the insensitivity of  $C_D$  on the  $L/D$  ratio. From  $L/D = 0.1$  to  $L/D = 7$  the  $C_D$  value drops only slightly from 0.85 to 0.8.

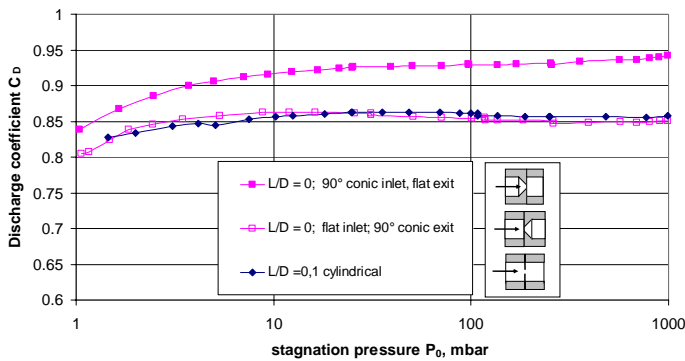


**Fig. 5 Subsonic inlet geometry and discharge coefficients**

The strong dependence of the contraction coefficient  $A_{eff}/A_{geom}$  on the nozzle entrance geometry is also demonstrated by the forward and backward tests of the nozzle 8 with  $L/D = 0$  and  $90^\circ$  conical entrance and flat  $180^\circ$  exit. The test results in Fig. 5 show that a  $90^\circ$  conical inlet geometry increases the high Reynolds number discharge coefficient from 0.85 to 0.94. In backward installation, this nozzle is flat faced with  $180^\circ$  cone angle and gives identical results as the cylindrical nozzle with  $L/D = 0,1$ .

### $C_D$ as function of Reynolds numbers

The measured discharge coefficient of all tested nozzles are shown in Fig 6 as function of stagnation pressure  $p_0$ . The discharge coefficient of short cylindrical orifices with  $L/D < 0,12$  is extremely insensitive to a  $Re$  reduction. It keeps its continuum value of  $C_D = 0.85$  for  $Re_D > 50$ . With increasing  $L/D$  the decrease of  $C_D$  is shifted to higher  $Re$  values and the sensitivity on  $Re$  is increased.

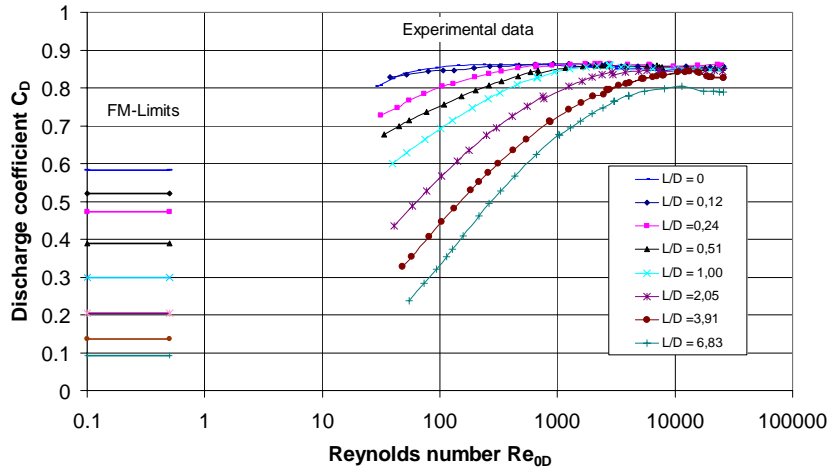


**Fig. 6 Discharge coefficient  $C_D$  as function of Reynolds number**

The figure contains, for each  $L/D$ , the corresponding free molecular limits calculated with Clausing's method. The data indicate that the viscous influence generates in its beginning a slight  $C_D$  maxima, which is continued by a strong decrease of  $C_D$  with decreasing Reynolds number. The relation  $Kn_{0,D} = 0.8741/Re_{0,D}$  shows that the experimental data cover a

regime with  $Re > 40$  or  $Kn > 0.02$ . For ideal orifices with  $L/D < 0.1$  the continuum value of  $C_D = 0.85$  is approximately valid for  $Kn_0 < 0.01$  or  $Re_{0,D} > 80$ . For large  $L/D$  the decrease of  $C_D$  due to viscous influence is shifted to higher Reynolds numbers. For  $L/D = 7$  the  $C_D$  decrease starts at a Reynolds number of 8 000.

### Correlation parameter for discharge coefficient reduction

The pressure drop of subsonic viscous flow in the entrance section of circular tubes is correlated by the following parameter  $Dp/q = \text{Function}(x/D/ReD)$ . We therefore tried a similar correlation approach which also considers the viscous  $L/D$  influence on the discharge coefficient. Figure 7 shows all experimental data evaluated according to this parameter. The evaluation shows that the parameter  $\sqrt{(L/D)/Re_D}$  correlates the discharge coefficient reduction extremely well. For sonic orifice flow, the relevant Mach number is  $Ma = 1$  and therefore the above correlation parameter is in principle a modified viscous parameter defined as  $V_{mod} = \sqrt{(L/D)Ma} / \sqrt{1/Re_D}$ . For the limiting case of  $L/D = 0$  the above correlation would fail. As no visible experimental difference of  $C_D$  for  $L/D = 0$  and  $L/D = 0,12$  exists, we introduced a minimum virtual  $L/D_{min} = 0.1$  for evaluation of the  $L/D = 0$  data.

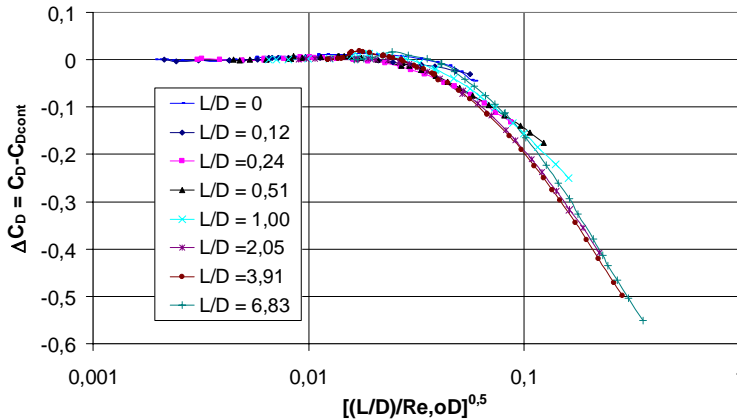


**Fig. 7 Reduction of Discharge coefficient  $\Delta C_D$  as function of correlation parameter  $[(L/D)/Re_0D]^{0,5}$**

## THE RESULTS OF ON AXIS FLOW FIELD MEASUREMENTS

These unpublished measurements were obtained during 1981 and 1982 in the DLR high vacuum facilities. In the frame of this study we only show the measurement obtained with nitrogen. Fig. 8 shows the results of the on-axis static pressure measurements  $p/p_0$  for 5 nozzles with  $L/D$  ranging between 0.1 and 2. The origin of the geometric coordinates system is the nozzle inlet plane. It is evident that with increasing  $L/D$  the flow acceleration is delayed.

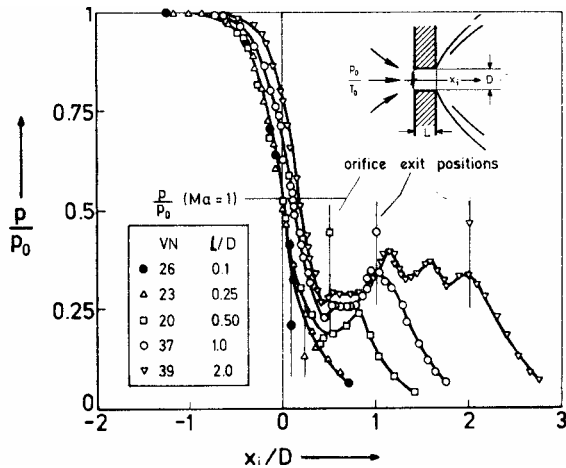


Fig. 8 shows the results of the on-axis static pressure measurements  $p/p_0$  for 5 nozzles with  $L/D$  ranging between 0.1 and 2. The origin of the geometric coordinates system is the nozzle inlet plane. It is evident that with increasing  $L/D$  the flow acceleration is delayed. This means the static pressure drop profile is shifted closer to the nozzle entrance plane. The initial profiles for  $1 > p/p_0 > 0.25$  are similar however shifted in the nozzle direction. In the figure we have indicated the pressure ratio  $p/p_0$  for  $Ma = 1$ . For  $L/D = 0.1$  and  $0.25$  the  $x/D$  position for  $Ma = 1$  is reached approximately at the nozzle entrance plane. With increasing  $L/D$  the sonic position  $x/D$  ( $Ma = 1$ ) moves further into the nozzle. For  $L/D = 0.5$  a first compression wave with a static pressure peak is observed

**Fig. 8 On-axis static pressure distribution through cylindrical orifices**

The location of this peak is downstream of the nozzle exit plane. For  $L/D = 1$ , the initial expansion in the cylindrical nozzle reaches a minimum value of  $p/p_0 = 0.23$  at  $x/D = 0.4$  which corresponds to a Mach number of  $Ma = 1.73$ . The compression peak is located at the nozzle exit plane. For  $L/D = 2$ , the  $Ma = 1$  position is reached at  $x/D = 0.2$  and several compression waves inside the nozzle can be observed.

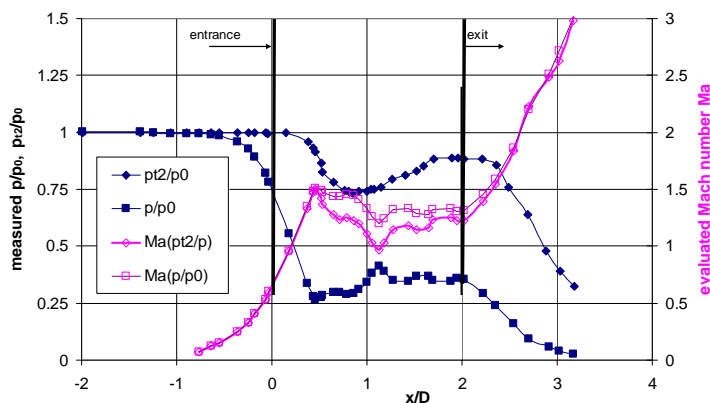
### The flow details in the $L/D = 2$ nozzle

For this nozzle we show the results of static and Pitot pressure measurements in Figure 9. From these measurements we can evaluate the Mach number in the following two ways:

- $Ma = \text{Function of } p/p_0$ , using isentropic relations between source chamber and local conditions.
- $Ma = \text{Function } p_{t2}/p$ , using the local measured quantities namely  $p$  and  $p_{t2}$  and the Rayleigh-Pitot formula.

This evaluation does not depend on the assumption of isentropic flow expansion.

Fig 9 shows on the left scale pressures and on the right scale Mach numbers. The flow passes the nozzle entrance plane with  $Ma = 0.7$ . A Mach number of 1 is reached at  $x/D = 0.2$ , the flow continues to expand and reaches, at  $x/D = 0.4$ , a maximum Mach number of  $Ma = 1.5$ . Up to this point we have isentropic expansion and the Mach numbers determined by both methods are identical. In the remaining nozzle section compression and expansion waves are observed which influence the Mach number.



observed which influence the Mach number. In addition different Mach profiles are evaluated in this nozzle section.

**Fig. 9 Measured and evaluated on axis flow properties in cylindrical nozzle with  $L/D = 2$**

The Pitot pressure method predicts a minimum Mach number of  $Ma = 1$  at  $x/D = 1.1$ . The flow leaves the nozzle with  $Ma = 1.25$  and continues its expansion as a free jet. In this expansion regime both methods give identical Mach numbers.

This indicates weak compression waves in the nozzle, causing only a negligible total pressure loss.

### Flow structure in the nozzles and discharge coefficients.

In the high Reynolds number regime the discharge coefficient is, in principle, determined by the effective sonic throat area. Due to the sharp inlet corners a flow separation with streamline contraction occurs at the nozzle inlet. This flow contraction due to separation is responsible for the effective sonic throat. The mass flow and the on-axis

flow profile showed that in the range  $L/D < 7$ , the sonic throat is determined by the entrance geometry. For  $L/D \ll 1$  the separation should be of the open type and the sonic throat will be located downstream of the orifice exit. The expansion through the nozzle will be free from compression waves. For  $L/D > 0.5$  a closed separation bubble seems to be formed at the entrance corner. This bubble forms the sonic throat and at reattachment compression waves will result. The static pressure measurement indicate this for  $L/D \geq 0.5$ .

The Fig. 9 explains this separation behavior. It should also be pointed out that the flow contraction ratio and the discharge coefficient can be strongly influenced by the nozzle inlet geometry. With an entrance cone of  $90^\circ$  (full angle) the discharge coefficient is increased from  $C_D = 0.85$  to 0.94 as shown in Fig. 5. In addition slight rounding of the entrance corner will influence the flow contraction and the discharge coefficient.

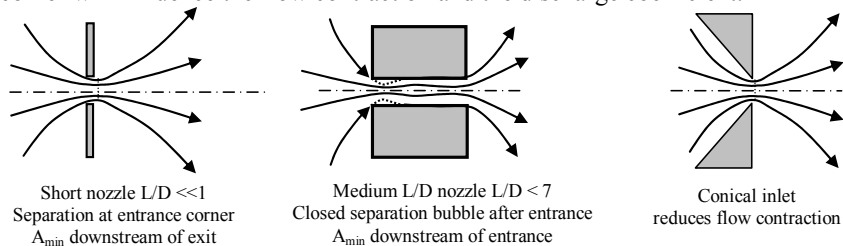


**Fig. 10 Sketch of flow contraction and separation bubble in cylindrical orifices**

## CONCLUSIONS

Cylindrical sonic orifices offer the advantage of simple manufacturing. Therefore small sonic orifices are often made in this way. In the continuum flow regime ( $Re_D > 10000$ ) the discharge coefficient depends only weakly on  $L/D$  and varies from 0.85 to 0.8. between  $L/D = 0$  to  $L/D = 7$ . In this  $L/D$  range, the entrance determines the flow contraction and the effective diameter. The sensitivity of the discharge coefficient is extremely small for  $L/D < 0.12$ . Almost constant  $C_D$  is obtained in the Reynolds number range between  $Re_D = 80$  and 25000. With increasing  $L/D$ , viscous effects decrease the  $C_D$  and the onset of this decrease is shifted from  $Re_D < 80$  for  $L/D = 0.12$  to  $Re_D = 80000$  at  $L/D = 7$ . The flow field measurements showed the inside flow structure in the nozzles. For  $L/D < 0.5$  an open separation at the entrance corner is observed and for  $L/D > 0.5$ , a closed separation bubble is formed, with the effective throat diameter located about 0.2 diameters behind the nozzle entrance.

## REFERENCES

- 1 Ashkenas K. Sherman F.S. *The Structure and Utilization of Supersonic Free Jets in Low Density Wind Tunnels* Rarefied Gas Dynamics, Suppl.3 Vol. 2, Academic Press 1966, pp 84- 1041
- 2 Anonym, *National Standards for Flow Metering*
- 3 Liepmann H.W. *Gas Kinetics and Gas Dynamics of Orifice Flow*, J. Fluid Mech.10 1961, pp 65-79
- 4 Naumann A., Chun C.H., *Mass Flow Measurements for Sharp Edged Orifices in Low density Flow*, Rarefied Gas Dynamics, Proc. 9<sup>th</sup> Int. Symp. DFVLR Press, 1974, pp. D21-1-D21-10, Edited. M Becker, M. Fiebig
- 5 Kulova N.M, Hosack G.A. *Supersonic Nozzle Discharge Coefficients at Low Reynolds numbers* AIAA Journal, Vol.9, 1971, pp1876-1879
- 6 Tang S. P. ,Fenn J. B. *Experimental Determination of the Discharge Coefficient for Critical Flow through an Axis-symmetric Nozzle*, AIAA Journal, Vol.16, 1978, pp 41-46
- 7 Sharipov F. , *Numerical simulation of rarefied gas flow through thin orifices* , J. Fluid Mech. Vol. 518, 2004, pp. 35-60
- 8 Clausing G., *Über die Strömung sehr verdünnter Gase durch Röhren beliebiger Länge* , Annalen der Physik, 5. Folge, Band 12, 1932, pp. 961-989
- 9 Sreekanth A. ,*Transition Flow through Short Circular Orifices* , Physics of Fluids, Vol. 8 1965 pp.1951-1956
- 10 Hansen M., *Düsen und Blenden bei kleinen Reynoldszahlen*, Forschung 4 Bd. 1933, Heft 2 pp. 64-66
- 11 Gimelshein S.F. et al., *Experimental and numerical modeling of rarefied gas flow through short tubes*, Rarefied Gas Dynamics, 24. Int. Symp. AIP Conf. Proceedings 762, ed. M. Capitelli, New York, 2005, pp. 437-443
- 12 Danilatos G.A., *Direct Simulation Monte Carlo Study of Orifice Flow*, Rarefied Gas Dynamics, 22. Int. Symposium, AIP Conf. Proceedings 585, ed. T. J. Bartel, M.A. Gallis, New York, 2001, pp. 924-932
- 13 Hefer, H., Koppenwallner G., Legge, H., Wuest W., *Eine hypersonische Windkanalanlage für kleine Gasdichten*, Forschungsbericht W 70-51, 1971 DFVLR